13 Particle physics with the CMS experiment at CERN

L. Caminada, F. Canelli, V. Chiochia, A. de Cosa, C. Favaro, C. Galloni, A. Hinzmann, T. Hreus, B. Kilminster, C. Lange, J. Ngadiuba, D. Pinna, P. Robmann, D. Salerno, S. Taroni, M. Verzetti, and Y. Yang

in collaboration with the:

CMS - Collaboration

Particle physics experiences a very exciting era. On July 4, 2012 the CMS and ATLAS experiments at the CERN LHC announced the discovery of a Higgs-like particle. After 48 years of desperate searches, the last missing ingredient of the Standard Model (SM) of particle physics may well have been found [1, 2].

Whether this indeed is the SM Higgs boson, or possibly one of several Higgs bosons predicted in some theories that go beyond the SM, remains to be seen. The LHC now enters a phase of studying the Higgs boson, measure its properties, including decay modes and additional interactions relating to a new physics scale. These tasks are among the primary goals and challenges of the next LHC run.

The Higgs boson provides a mechanism for mass generation of fundamental particles and electroweak symmetry breaking. Nevertheless, with the existence of a 126 GeV Higgs boson, the question of the stability of its mass has now become urgent. Unless there is an incredible and delicate fine-tuning of the SM, there must be new particles with masses around a TeV that produce loop corrections with the necessary cancellations to stabilize the Higgs boson mass. Theoretical models such as supersymmetry (SUSY) and warped extra dimensions address these and other issues. If these TeV-mass particles exist, the new energy regime of the LHC will allow us to directly produce them and observe their interactions and properties.

Even though the SM describes our universe at the shortest distance scale, it fails extraordinarily at the largest distance scale. Cosmological and astronomical observations have revolutionized our view of the universe by uncovering the existence of dark matter, the vanishingly small relative strength of gravity, the accelerating expansion of the universe, and the matter-antimatter asymmetry. The SM is unable to accommodate any of these observations.

If dark matter is indeed a stable neutral weakly interacting particle with mass less than around a TeV as expected, we must produce it at the LHC. If the relative strength of gravity can be explained, for instance by a universe comprised of both TeV-scale and gravity-scale branes, then new particles will be produced at the LHC. Therefore, the LHC may well bridge the gap between the shortest and the largest distance scales.

[1] CMS collaboration, Phys. Lett. B **716** (2012) 30.
[2] ATLAS collaboration, Phys. Lett. B **716** (2012) 29.

13.1 CMS

CMS [1, 2] is a multipurpose detector designed for a variety of particle physics studies at the LHC. The LHC delivered proton collisions until February 2013 concluding the first three-year running period and entering a two-year shutdown period (Long Shutdown 1, LS1). During this first period CMS collected an integrated luminosity of 23.3 (6.1) fb^{-1} at the center-of-mass energy $\sqrt{s} = 8$ (7) TeV. The large datasets are currently being analyzed. In parallel, LS1 activities are planned until end 2014. LHC is expected to restart operations in early 2015 with proton beams colliding at the center-of-mass energy of 13 TeV.

CMS consists of different detector layers (see Fig. 13.1). An all-silicon tracker, an electromagnetic calorimeter, and a hadronic sampling calorimeter are all contained within a large-bore 3.8 T superconducting solenoid. Beyond the solenoid are four layers of muon detectors. The CMS tracker is composed of the inner pixel detector and the outer silicon strip detector. The pixel detector consists of three barrel layers (BPIX) at 4.4, 7.3, and 10.2 cm, and two forward/backward disks (FPIX) at longitudinal positions of $\pm$34.5 cm and $\pm$46.5 cm and extending in radius from about 6 to 15 cm.

The high segmentation of the pixel detector permits the building of seed clusters for the tracking algorithm reconstruction and also for the fast online track reconstruction in the high level trigger (HLT). The pixel detector is used for electron/photon identification and muon reconstruction, but its precision resolution is crucial for primary vertex and pile-up vertex reconstruction, and identification of long-lived τ-leptons and B-hadrons traveling a few millimeters before decaying. The performance of the current pixel detector during data taking has been excellent. It is noteworthy that the BPIX was built by the CMS Swiss Consortium: PSI, ETH and the University of Zürich.

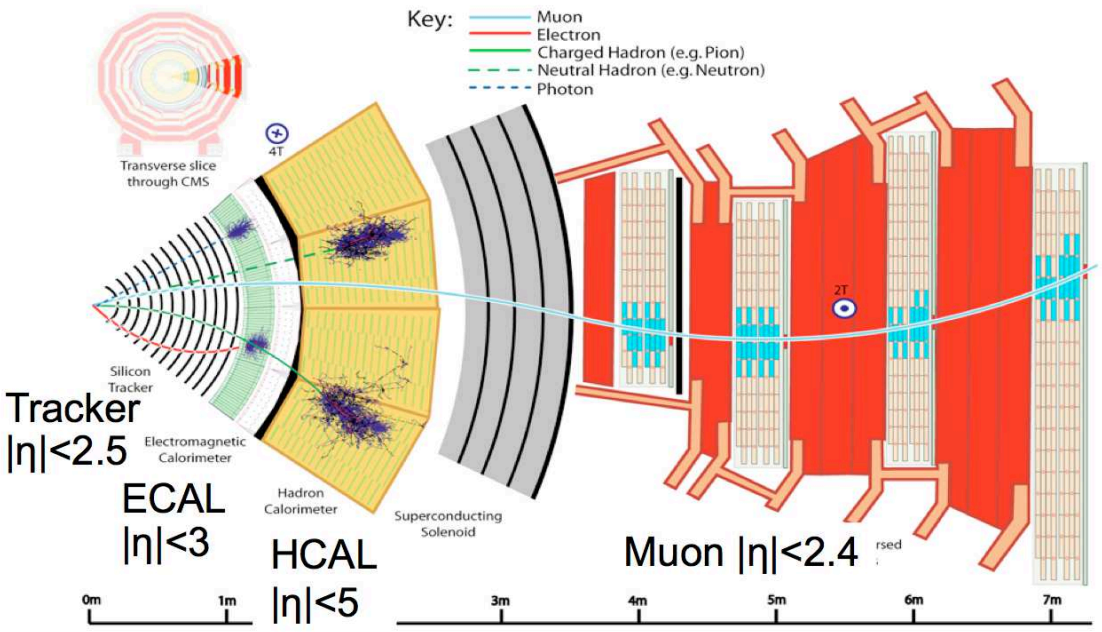

FIG. 13.1 – Schematic view of a sector of the CMS detector, illustrating how muons, electrons, charged hadrons, neutral hadrons and photons are reconstructed.

Members of our group cover important coordination roles within the CMS collaboration. A. de Cosa is the level3 online pixel coordinator, A. Hinzmann is co-convener of the Exotica in jet final states physics group, B. Kilminster is co-convener of the phase 2 upgrade future Higgs physics group, T. Hreus coordinates the Tracker Detector Performance Group, in charge of the tracker offline software and operations, M. Verzetti was editor of the analysis note detailing the searches for associated W/Z bosons and Higgs production in τ decays, while V. Chiochia is a member of the CMS conference committee and B-physics steering group. Most of our group have served as referees of several recent publications. Currently F. Canelli holds the position of group leader.

More than hundred publications were released by the CMS collaboration in the period covered by this report. In what follows, we describe the contributions of our group, which were focused in three main areas of research: physics measurements and searches, analysis techniques that benefit these physics analyses, and the operation and upgrade of one of the detectors vital to these measurements.

[1] *CMS technical design report*, CMS collaboration, CERN-LHCC 2006-001.

[2] S. Chatrchyan *et al.* [CMS Collaboration], JINST **3**, S08004 (2008).

13.2 Measurements and searches

In this subsection, we highlight physics analyses and other contributions we have been engaged in. A primary physics focus was on the better understanding of the Higgs sector. We also searched for new particles motivated by dark matter, the MSSM, and extra dimensions, which could be in reach of LHC energies and luminosities.

13.2.1 Evidence of Higgs boson decaying to τ leptons

It is essential to determine the properties of the discovered particle with some accuracy to establish if it corresponds to the Higgs boson of the SM or of an extended model. The first evidence for the Higgs boson was reported in decays to boson pairs, such as W^+W^-, ZZ and $\gamma\gamma$. At the Tevatron, evidence was found for the Higgs decay to fermions in $H \to b\bar{b}$ [1]. Until recently, no such evidence was reported at the LHC. Decays to τ pairs are a promising channel because of the large event rate expected in the SM compared to the other leptonic decay modes and the smaller background with respect to $b\bar{b}$.

Our group has searched for the SM Higgs boson in the process $pp \to WH \to \ell\nu\tau_\ell\tau_{\rm had}$, where τ_ℓ and $\tau_{\rm had}$ indicate leptonic and hadronic τ decays, respectively. While this production mode has a lower cross section than the direct production channels, such as gluon-gluon fusion, it has a smaller background and may allow a more accurate measurement of the coupling constant.

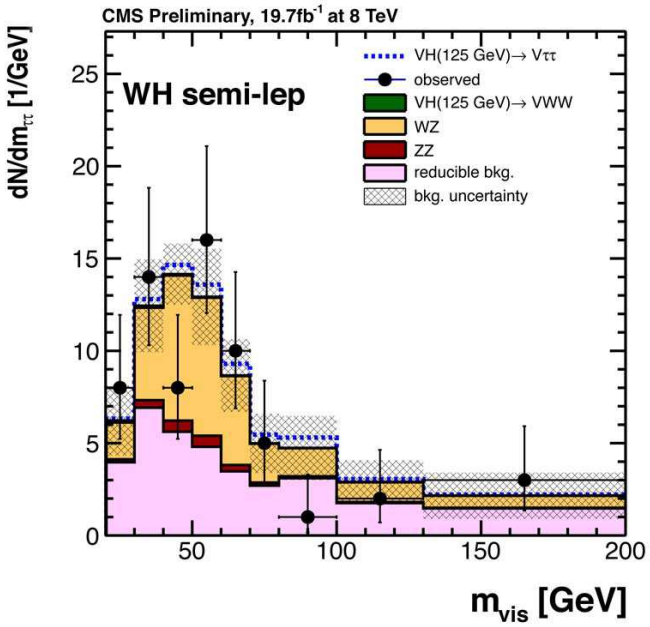

FIG. 13.2 –
The expected and measured $e\mu\tau_{\rm had}$ and $\mu\mu\tau_{\rm had}$ visible invariant mass for the 8 TeV data. The dashed line represents the expected contribution from $pp \to WH$ production.

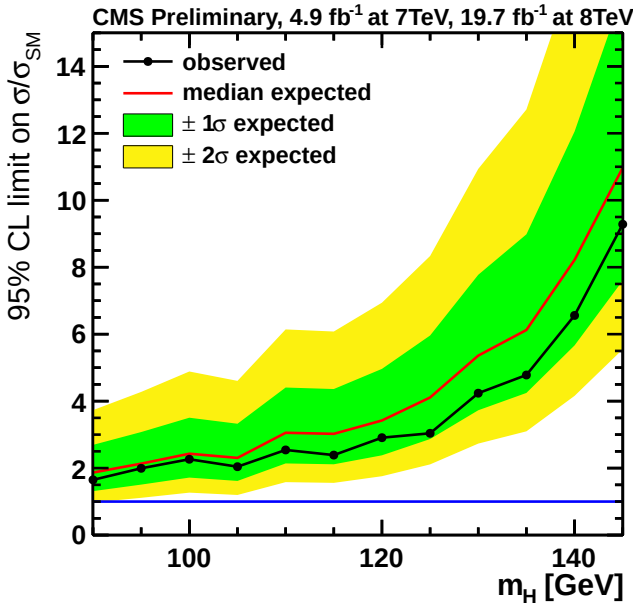

FIG. 13.3 –
Expected and observed 95% C.L. upper limits on SM Higgs boson production for the WH process.

The data analysis was based on 5 (19.7) fb^{-1} collected at 7 (8) TeV. Three final states were considered, where the undetected neutrino from the W decay was contributed to the missing transverse energy in the event: $\mu\mu\tau_{\rm had}$, $e\mu\tau_{\rm had}$, and $ee\tau_{\rm had}$. Results from the first two channels were fully scrutinized and included in the CMS journal article [2]. The $\ell\tau_\ell\tau_{\rm had}$ backgrounds were into two categories: irreducible WZ and ZZ diboson backgrounds with at least three genuine isolated leptons in the final state, and reducible "misidentified" backgrounds where at least one lepton candidate is a quark or gluon jet misidentified as a τ. The irreducible diboson backgrounds were estimated using Monte Carlo (MC) simulation while the misidentified backgrounds were estimated from data using a k-Nearest Neighbor classifier.

Events were selected with leading (sub-leading) leptons with $p_T > 20$ (10) GeV/c and $\tau_{\rm had}$ candidates with $p_T > 20$ GeV/c. The leptons were required to have the same charge to reduce the Drell-Yan and $t\bar{t}$ backgrounds. Given the high correlation of misidentification probability and lepton transverse momenta, events passing the selection were further divided into two categories according to the scalar sum of the p_T of the three final state objects. The visible invariant mass of the final state is shown in Fig. 13.2. The measured distribution is consistent with the sum of all backgrounds and no significant excess is observed. Expected and observed exclusion limits were calculated in the CL$_s$ approach as a function of the Higgs candidate mass and found to be consistent, as shown in Fig. 13.3.

The channels analyzed by our group were found to be the most sensitive at low mass among the final states in which a Higgs boson is produced in association with a W or Z and help improving the overall sensitivity of the CMS searches in τ decays when combined to other channels. Results obtained in the WH and ZH channels were combined with the inclusive $H \to \tau\tau$ searches, including six more decay channels [2]. The combination resulted in a broad excess of events above the background expectation with a local significance above three standard deviations in the mass range between 115 and 130 GeV/c^2, as shown in Fig. 13.4. Assuming the excess to be due to $H \to \tau\tau$ signal leads to a measured mass of $m_H = 122 \pm 7$ GeV, which is consistent with previous measurements. The best fit of the observed $H \to \tau\tau$ signal cross section for $m_H = 125$ GeV/c^2 is 0.78 ± 0.27 times the SM expectation. These observations constitute the first direct evidence for the 125 GeV/c^2 Higgs boson decaying to a pair of τ leptons.

13.2.2 Higgs boson couplings to top quark pairs

Higgs decays involving top quarks will bring invaluable information since the very large top mass results leads to the full strength of the Higgs boson coupling. The magnitude of this coupling can be directly measured through the cross section of Higgs boson production in association with a top pair. We are leading a search for $t\bar{t}H$, where at

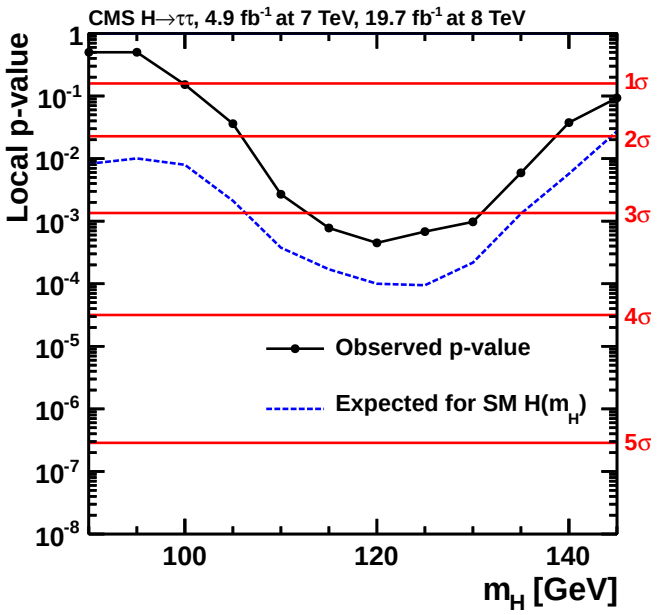

FIG. 13.4 – Local p-value and significance in number of standard deviations as a function of the SM Higgs boson mass hypothesis for the combination of all decay channels.

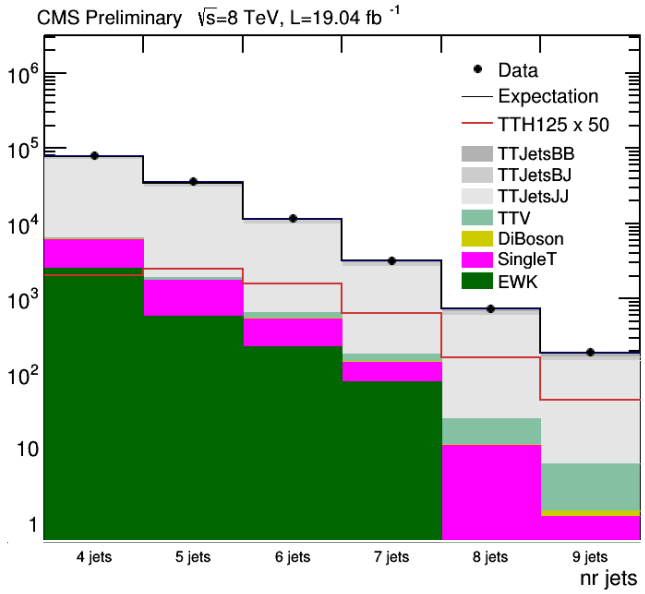

FIG. 13.5 – Multiplicity of jets in SL events with $N_j \geq 4$ and at least two jets passing a medium CSV (b-tagger) cut.

least one of the top-quarks decays leptonically through $t \to bW$, with $W \to \ell\nu_\ell$, $\ell = e, \mu$, whereas one W decay may proceed hadronically, with $W \to q\bar{q}$. The $t\bar{t}H$ production channel comes with experimental challenges due to its small cross section and high QCD background rates. The $H \to b\bar{b}$ decay channel is the most promising thanks to its large branching ratio and to the high efficiency of tagging jets from b-quark hadronization. Nevertheless, the QCD background $pp \to t\bar{t} + b\bar{b}$ remains irreducible with respect to b-tagging, and it has a much larger cross section than the signal [3].

The Matrix Element Method (MEM) [4] provides an optimal separation of signal and background by exploiting both the experimental information and the theoretical model in assigning weights under competing hypotheses. The method also reduces combinatorial self-background arising from matching reconstructed jets to the four b-quarks from the Higgs and top-quark decays. The method calculates the probability $w_i(\mathbf{y}|\lambda)$ of measuring a set of observables $\mathbf{y}$ under a hypothesis i, given model parameters λ. The ratio $w_0(\mathbf{y}|\lambda)/w_1(\mathbf{y}|\lambda)$ provides a good separation between signal and background (i=0,1). The probably density is given by

$$w_i(\mathbf{y}|\lambda) = \frac{1}{\sigma_i(\lambda)} \int_\Omega d\mathbf{x} \int dx_a dx_b \Phi(x_a, x_b) \times \delta^4((x_a P_a + x_b P_b) - \sum \mathbf{p}(\mathbf{x})) |\mathcal{M}_i(\mathbf{x}|\lambda)|^2 W(\mathbf{y}|\mathbf{x}, \lambda)$$

The integration is performed over the phase-space of the final state particles $\mathbf{x}$ and over the momentum fractions $x_{a,b}$ of the initiating partons in the infinite momentum frame of the colliding protons which have 4-momenta $P_{a,b} = (\sqrt{s}/2, 0, 0, \pm\sqrt{s}/2)$. The integrand includes the parton flux factor Φ, the scattering amplitude of process i squared $|\mathcal{M}_i|^2$ and the transfer function W, which gives the probability density of measuring a set of observables $\mathbf{y}$ given a phase space point $\mathbf{x}$.

In our analysis, the integral is computed numerically using the `VEGAS` [5] algorithm for each possible quark-to-jet association (permutation) and then summed to give the final probability. The scattering amplitude is evaluated numerically at LO accuracy by the program `OpenLoops` [6] and the narrow width approximation is used to calculate the intermediate particle propagators. The transfer function is determined by the detector characteristics and performance.

Our analysis uses the 8 TeV data from 2012 corresponding to 19.04 fb^{-1}. Events are separated depending on the lepton and jet multiplicities to take advantage of the different signal to background ratio. Single-lepton (SL) and double-lepton (DL) events contain exactly one lepton or an opposite-sign lepton pair, respectively. Figure 13.5 shows the jet multiplicity in the SL channel.

A further selection is applied based on the b-tagger discriminator ξ of jets. For each event, the jet collection is sorted based on ξ and a b-tag likelihood ratio b_{LR} is calculated, which optimally separates the hypotheses that exactly four or two jets originate from b-quarks. Signal events as well as those from the irreducible $t\bar{t} + b\bar{b}$ background contain four b-quarks and thus have a value of

b_{LR} close to 1.0, while those backgrounds containing light quarks have a value closer to zero. A cut is made on b_{LR} depending on the channel and the number of jets. The low purity region is dominated by $t\bar{t} + jj$ and deficient in the signal, and thus provides a good control region. Events passing the b_{LR} selection are further classified into categories to take advantage of the differences between signal and background.

A number of tests to verify the algorithm have been performed. In all cases the MC is found to reproduce the data to within acceptable limits. We are currently in the final stages of completing the 8 TeV analysis and have yet to un-blind the data in the signal region.

The expected 95% CL upper limit on the signal strength modifier $\mu = \sigma_{\mathrm{SM}}/\sigma$ with its $\pm 1\sigma$ and $\pm 2\sigma$ uncertainties have been determined for each category. The combined result is $\mu < 2.9$.

We have found an encouraging improvement of 20% with respect to the analysis done previously by CMS. More improvements have been included to this analysis. The analysis is still under approval by the CMS collaboration and the final version is expected to be released during 2014.

13.2.3 MSSM Higgs boson search

The light SM Higgs boson mass demands a mechanism for its stabilization, since naively radiative corrections should make it many orders of magnitude larger. One such mechanism, SuperSymmetry (SUSY), provides loop corrections to the Higgs boson mass that cancel the loops from known SM particles. Within the MSSM (Minimal Supersymmetric Model), there are four additional heavier Higgs bosons (two oppositely-charged scalars, one neutral scalar, and a neutral pseudoscalar) which should be detectable at the LHC since the favored masses are just above current limits. Our group is searching for neutral Higgs bosons decaying to $b\bar{b}$ produced via the MSSM in association with a b-jet. This is a process whose cross section is enhanced compared to SM $H \to b\bar{b}$ production by a factor of $\tan^2(\beta)$, which could be as large as a 1000.

For $\tan^2(\beta) \geq 3$ the decay to $b\bar{b}$ is the dominant Higgs decay channel with a branching ratio of about 90%. A previous search was done with 7 TeV, setting limits on the MSSM Higgs mass up to 350 GeV [7], which set the most stringent bounds on MSSM Higgs-production in this final state. Since higher MSSM Higgs boson masses are now accessible with 8 TeV, $H \to b\bar{b}$ becomes more boosted, and the fraction of events for which two B-hadrons are merged into a single jet is significant. Our group has found that sensitivity is improved by evaluating these events separately. We have investigated sensitive variables (secondary vertex variables, such as vertex mass) to discriminate single-b from two-b jets and introduced a new discriminant for increasing the sensitivity of the analysis significantly. Dedicated triggers, which perform online b-tagging based on impact-parameter significance are employed to cope with the large hadronic interaction rate at the LHC. Based on these, different mass ranges have been defined for the new data, for which we have optimised the event selection. Furthermore, we have evaluated the non-QCD-multijet background events, and estimated the systematic uncertainties for the analysis.

The new discriminant that we have developed, called event b-tag, is essential to get a handle on the background composition. Since the background consists largely of QCD multi-jet events, the background model is taken from data, where the different flavour fractions are determined from double-b-tag events. A full 2D maximum likelihood fit to the invariant mass of the leading two b-jets and the event b-tag is used to determine the event yields. A potential signal would show up as a bump in the invariant mass spectrum and be a clear sign of physics beyond the Standard Model. The result analyzing the full 2012 dataset with 8 TeV is entering CMS review shortly and will soon be published. We will continue to update this search with the 13 TeV run, which will access a new MSSM Higgs boson mass range.

13.2.4 Study of $pp \to Zb\bar{b}$ production

The production of b-quark pairs in association with Z bosons in the process $pp \to Zb\bar{b}$ is the main SM background to Higgs boson searches in b-quark decays and other searches for new physics. SM predictions at next-to-leading order accuracy have been performed assuming massive or massless b quarks, usually referred as four- and five-flavour calculation schemes, respectively. The validation of the different calculation techniques is of great importance for the correct background estimates in future searches.

Our group performed the first measurement of the total cross section and angular correlations of B hadrons produced in this process, using a data sample corresponding to an integrated luminosity of 5 fb^{-1} at $\sqrt{s} =$ 7 TeV [8]. B hadrons were identified through the displaced vertices from their decays, using the inclusive vertex finder (IVF). The IVF technique [9] is independent from jet reconstruction and allows the full angular range to be probed, including configurations with collinear B hadrons. Figure 13.6 shows distributions of the kinematic variable ΔR_{BB} defined as:

$$\Delta R_{BB} \equiv \sqrt{(\Delta\eta_{BB})^2 + (\Delta\phi_{BB})^2} \ ,$$

with η the pseudorapidity and ϕ the angle in the transverse plane. The cross sections were evaluated in several regions of the Z boson transverse momentum.

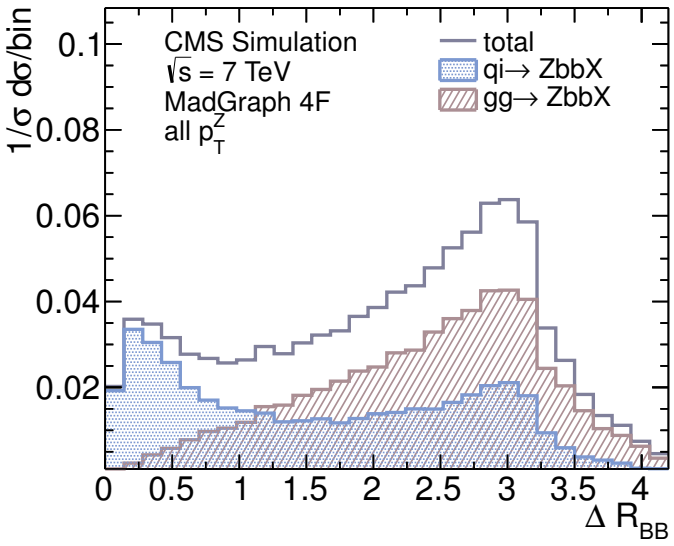

FIG. 13.6 – Distributions of ΔR_{BB} as predicted by MADGRAPH MC. The separate components from $gg \to Zb\bar{b}$ and $qq, qg \to Zb\bar{b}$ are indicated.

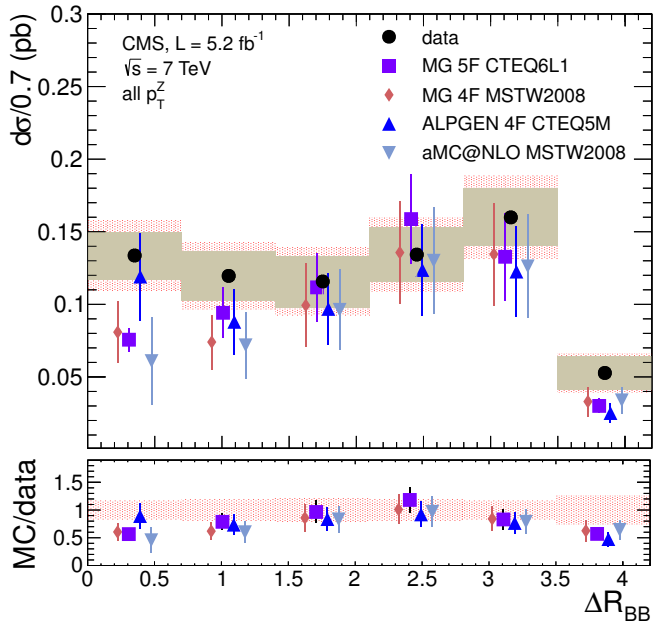

FIG. 13.7 – Differential cross section as a function of ΔR_{BB}. CMS data are compared with hadron-level predictions in the four- and five-flavor schemes, and for NLO QCD.

The measurements were compared with MC simulations implementing different flavour number schemes, as shown in Fig. 13.7. The ΔR_{BB} distribution indicates that the four-flavor prediction implemented in ALPGEN provides the best description of CMS data with five-flavour and NLO predictions below the data for low angular separations. Furthermore the total hadron-level cross section is systematically larger than MC predictions, partly because of the excess in the collinear ΔR_{BB} region.

13.2.5 Search for dark matter particles with top quarks

A popular candidate for dark matter is the weakly interacting massive particle (WIMP), which arises naturally in several models beyond the SM, like supersymmetry. So far, however, there is no established knowledge about its nature and properties, including its mass and interactions with ordinary matter [10, 11].

With minimal assumptions, the interaction Lagrangian between dark matter particles and quarks can be described by an effective field theory (EFT),

$$\mathrm{L_{int}} = C\,(\bar{q}\Gamma^q q)(\bar{\chi}\Gamma^\chi \chi)\ ,$$

where C represents the coupling constant, which usually depends on the mass of the dark matter particle M_χ and the scale of the interaction M_*, and the operator Γ describes the type of the interaction, including scalar ($\Gamma = 1$), pseudoscalar ($\Gamma = \gamma^5$), vector ($\Gamma = \gamma^\mu$), axial vector ($\Gamma = \gamma^\mu\gamma^5$) and tensor interactions.

The exact form of the constant C depends on the particular type of the interaction considered. In the case of a scalar interaction, the coupling strength is proportional to the mass of the quark,

$$\mathrm{L_{int}} = \frac{m_q}{M_*^3}\bar{q}q\bar{\chi}\chi$$

which means couplings to light quarks are suppressed and traditional inclusive mono-jet searches are not very sensitive [12–15].

We performed a search in the di-lepton channel [16], selecting events with large transverse missing energy ($\not\!\!E_\mathrm{T}$) and at least two jets. No excess was found above SM expectations and we set the first cross section limits on this process. Cross sections higher than 0.09 to 0.31 pb are excluded at the 95% Confidence Level (CL) for M_χ ranging from 1 GeV to 1 TeV. These results translate into new lower limits on M_*, as shown in Fig. 13.8.

Moreover, in the last part of the year we have developed this analysis in the single-lepton and fully hadronic channels. Both channels are expected to improve about 30% of the search sensitivity on the interaction scale.

In addition to top quarks, dark matter can also be produced in association with bottom quark pairs, providing a striking search signature. Dark matter signals are manifested in events with large $\not\!\!E_\mathrm{T}$, one or two b-tagged jets and with no other significant activities recorded in the detector. No results are available yet but the channel has a sensitivity similar to the previous one.

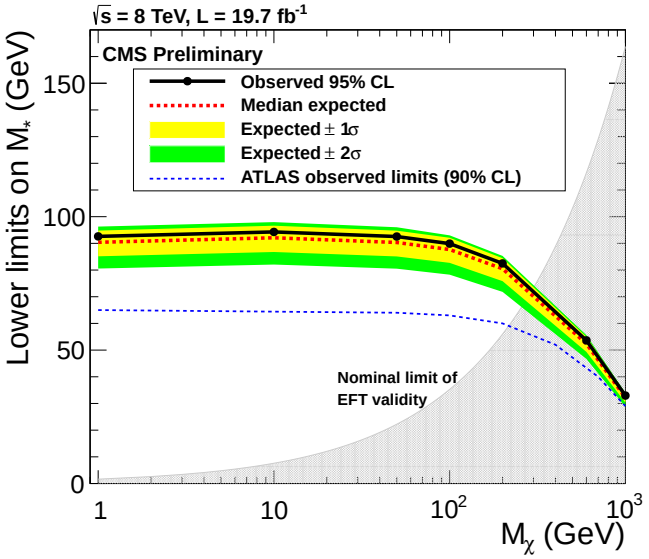

FIG. 13.8 – Observed exclusion limits in the plane of dark matter mass M_χ and interaction scale M_*. The region below the solid curve is excluded at 95% CL. The previous most stringent 90% CL limits (from ATLAS) are also shown. The results expected for 1σ and 2σ fluctuations of the background are indicated. Under typical assumptions, the EFT considered in this analysis is expected not to be valid in the shaded area where $M_\chi^2 > 4\pi^2 M_*^3/m_t$.

[1] T. Aaltonen *et al.* [CDF and D0 Collaborations], Phys. Rev. Lett. **109**, 071804 (2012)

[2] S. Chatrchyan *et al.* [CMS Collaboration], *Evidence for the 125 GeV Higgs boson decaying to a pair of τ leptons*, arXiv:1401.5041 [hep-ex].

[3] A. Bredstein, Phys. Rev. Lett. **103**, (2009) 012002.

[4] DØ collaboration, Nature 429, 638-642 (2004); DØ collaboration, Phys. Lett. B **617** (2005) 23; *Helicity of the W boson in single-lepton $t\bar{t}$ events*, M.F. Canelli; FERMILAB-THESIS-2003-22. DØ collaboration, Phys. Lett. B **617** (2005) 23; CDF collaboration, Phys. Rev. Lett. **101** 252001 (2008); CDF collaboration, Phys. Rev. Lett. **103** 092002 (2009); CDF collaboration, Phys. Rev. Lett. **105** 042002 (2010); CDF collaboration, Phys. Rev. Lett. **99** 182002 (2007); CDF collaboration, Phys. Rev. D **84** 071105(R) (2011); CDF collaboration, Phys. Rev. Lett. **103** 101802 (2009); CDF collaboration, Phys. Rev. D **85** 072001 (2012).

[5] G.P. Lepage, Journal of Computational Physics **27** (1978) 192-203.

[6] F. Cascioli, Phys. Rev. Lett. **108**, (2009) 111601.

[7] S. Chatrchyan *et al.* [CMS Collaboration], Phys. Lett. B **722**, 207 (2013).

[8] S. Chatrchyan *et al.* [CMS Collaboration], JHEP **1312** (2013) 039.

[9] V. Khachatryan *et al.* [CMS Collaboration], JHEP **1103** (2011) 136.

[10] *Planck 2013 results. XVI. Cosmological parameters*, Planck Collaboration, arXiv:astro-ph/1303.5076.

[11] V. Trimble, Ann. Rev. Astron. Astrophys., **25** (1987) 425; E. Komatsu *et al.*, Astrophys. J. Suppl., **192** (2011) 18; J. L. Feng, Ann. Rev. Astron. Astrophys., **48** (2010) 495.

[12] J.M. Beltran *et al.*, JHEP **17** (2010) 1.

[13] J. Goodman *et al.*, Phys. Lett. B **695** (2011) 185; J. Goodman *et al.*, Phys. Rev. D, **82** (2010) 116010; P. J. Fox *et al.*, Phys. Rev. D **85** (2012) 056011; P. J. Fox *et al.*, Phys. Rev. D **86** (2102) 015010; Rajaraman *et al.*, Phys. Rev. D **84** (2011) 095013; T. Lin, E.W. Kolb, and L.-T. Wang, Phys. Rev. D **88** (2013) 063510.

[14] *Search for new physics in monojet events in pp collisions at $\sqrt{s}$= 8 TeV*, CMS collaboration, Tech. Rep. CMS-PAS-EXO-12-048, 2012.

[15] ATLAS collaboration, JHEP, **1304**, 2013; *Search for new phenomena in monojet plus missing transverse momentum final states using 10fb^{-1} of pp collisions at $\sqrt{s}$=8 TeV with the ATLAS detector at the LHC*, ATLAS collaboration, Tech. Rep. ATLAS-CONF-2012-147, CERN, Nov 2012.

[16] S. Chatrchyan *et al.* [CMS Collaboration], CMS-PAS-B2G-13-004.

13.3 New heavy particle searches in CMS

13.3.1 Search for heavy resonances in the W/Z-tagged dijet mass spectrum

One of the unsolved mysteries of the standard model of particle physics is why the strength of the electroweak force and gravity differ by 36 orders of magnitude. The model of large extra dimensions [1], where the gravitational force is allowed to propagate in extra spatial dimensions otherwise invisible to us, can explain this difference. At the same time, this model predicts the production of heavy graviton resonances decaying to pairs of particles in the visible dimensions, accessible with the highest energies of the LHC.

We search the data collected by the CMS detector in 2012 for new heavy particles decaying to pairs of W or Z bosons [2] as predicted by the large extra dimensions model. This final state is favored by extensions of the model in which the decay to lepton and photon pairs is suppressed[3]. The decay modes are also interesting since they are accessible only through novel jet substructure techniques which require a deep understanding of the jet substructure.

W and Z bosons decay predominantly into quarks which transform into jets. For the heavy resonances reachable at the LHC, the bosons have such large mo-

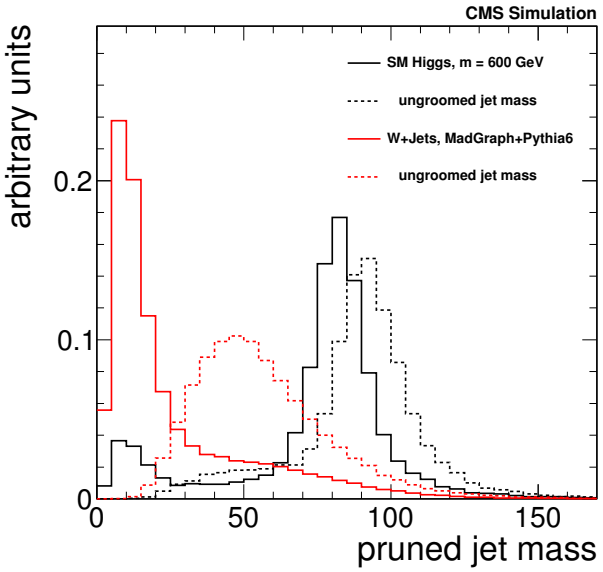

FIG. 13.9 – Simulation of the single-jet mass distribution for a heavy resonant signal and for the background, before and after pruning (see text).

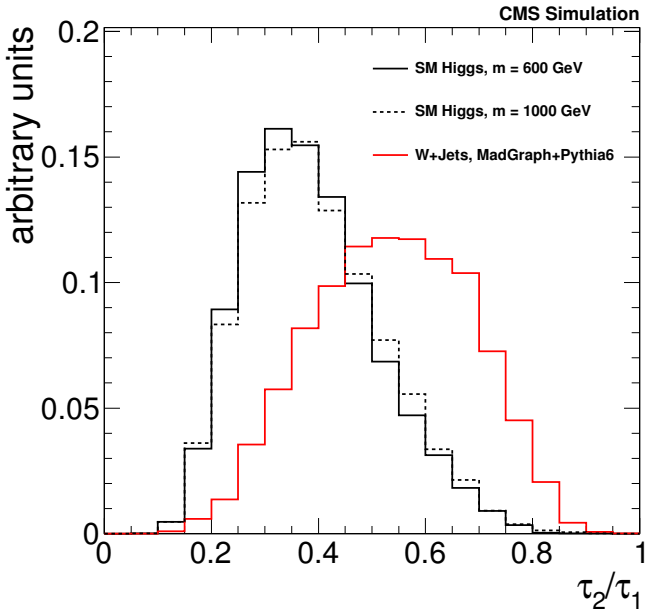

FIG. 13.10 – Distributions of the ratio τ_2/τ_1 for Higgs signal and background after requiring a pruned mass between 60 and 120 GeV. τ_2/τ_1 is a measure of the probability for two sub-jets rather than one.

menta that their decay products merge into a single jet. It is still possible to identify the W and Z bosons by studying the substructure of these merged jets. In recent years these W/Z-tagging algorithms have undergone a fast development. We have studied a variety of new algorithms identified the best one, the so-called pruning algorithm[4], which is based on the Lorentz invariant jet mass. The algorithm removes particles with background-like QCD radiation shown in Fig. 13.9, while keeping the particles from the quarks originating in W/Z decay. Additional selectivity is achieved by considering the N-subjettiness[5], which is a measure of the number of hard quarks in the jet (see Fig. 13.10).

Our ultimate W/Z-tagging algorithm [6] was calibrated with events of top pair production, which contain jets from W bosons with high momentum, and applied in the most recent CMS searches. Once W/Z bosons were identified, we searched for resonances on top of a smoothly falling background (Fig. 13.11). No signal was observed and the exclusion limits [2] are the most stringent to date for particles decaying to WW and reach up to 1.2 - 3.2 TeV depending on the model.

Presently, we focus on improving the reconstruction of jet substructure. By optimizing the calorimeter cluster algorithm, we managed to push the breakdown of reconstruction performance of boosted boson tagging due to detector resolution from p_T = 1 TeV to p_T = 1.5 TeV. By improving the use of the granularity of the electromagnetic calorimeter in the particle flow algorithm we were able to maintain the reconstruction performance up to p_T = 3.5 TeV, as needed for LHC Run II.

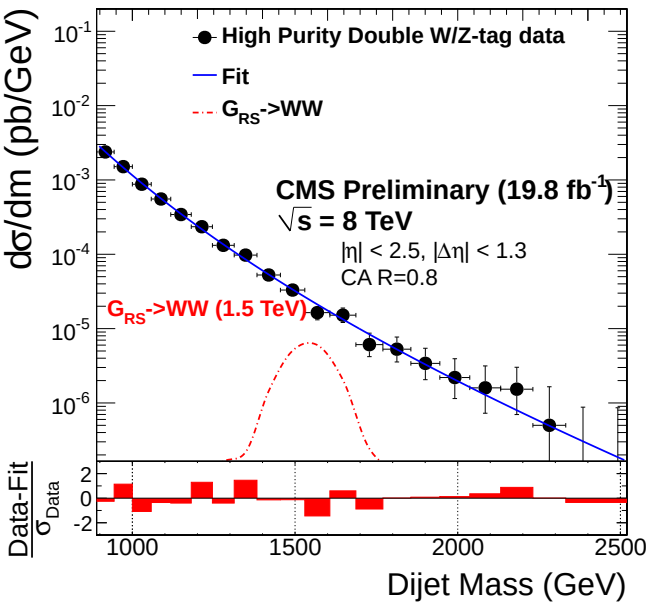

FIG. 13.11 – The final jet mass distribution fit for a signal-like resonance. No signal is observed, and upper limits on the cross-section are set.

13.3.2 Search for new heavy bosons with b-tagged jets and tau leptons in the boosted regime

In many extensions of the SM the spontaneous breaking of the electroweak symmetry is associated with new dynamics at the TeV scale, the origin of which may be new interactions [7] or compositeness [8]. Both concepts pre-

dict new resonances that mainly couple to pairs of massive bosons. Composite Higgs Models [9] provide a plausible solution to the hierarchy problem and consider the Higgs boson as a pseudo Nambu-Goldstone boson that couples to the SM particles and to new heavier gauge boson (Z' and W'). The existence of W' or Z' was postulated already in Grand Unification Theories but without predictions for their mass. A mass in the TeV region, accessible at the LHC, would solve the hierarchy problem. W' and Z' decay in these scenarios primarily to heavy particles, such as W , Z and Higgs bosons.

The first channel we are investigating $W' \rightarrow WH$, where the final state signature is given by a leptonic decay of the W and the hadronic decay of the Higgs into two b-quarks. For a W' mass between 1 and 3 TeV, the decay products are highly energetic ("boosted"), such that the final decay products can be difficult to separate. Hence the signature is characterized by a high p_T isolated lepton, large missing transverse energy and two high p_T jets from the b-quarks hadronization. In particular, the two b-jets from the Higgs are expected to merge into a single jet. The jet pruning and n-subjettiness algorithms mentioned previously may discriminate signal and background. Furthermore, the presence of b-quarks in the final state can be exploited to further suppress the background associated with light quark jets.

Our analysis is one of the first attempts to look for exotic final states with a Higgs boson, and indicates that astrongly coupled vector resonance with mass up to 1.5-2 TeV woulkd be detectable. The procedures are presently being developped with the 8 TeV data, with the aim of gaining enough experience to repeat the study with the 14 TeV data expected in 2015 when techniques for resolving boosted $H \rightarrow b\bar{b}$ become even more important and when higher luminosities and beam energies will extend the mass reach.

For boosted $H \rightarrow b\bar{b}$, b tagging, based on precise vertex reconstruction from the pixel detector to identify long-lived b quark decay, is reconsidered. We have produced a study [10] on the performance of CMS b-tagging algorithms in identifying jets containing two b quarks. We have investigated five different b-tagging algorithms, and considered multiple jet cone sizes, and jet-track association cone sizes. Our study showed the most commonly used multivariate algorithm, the Combined Secondary Vertex algorithm [11], was strongly outperformed by a more primitive algorithm, the Jet b Probability Algorithm [12], currently not used by CMS. This showed a need to make b-tagging in CMS to more sensitive to jets containing multiple b quarks.

Our group is also searching for heavy resonances, denoted as X, in the decays $X \rightarrow ZH$ and $X \rightarrow HH \rightarrow b\bar{b}\tau\tau$. The Higgs boson couples to fermions proportionally to their mass and therefore decays primarily to b quarks and secondarily to τ leptons. Since the decay to b quarks is obscured by a large QCD multi-jet background, having one Higgs boson decay to τ leptons is more promising since its backgrounds are mainly from W and Z decays.

The hadronic τ identification is performed by algorithms based on jet reconstruction with particle-flow techniques [13]. In the case of boosted taus decaying into three charged hadrons the tracks tend to overlap. For these cases we have studied discriminators based on the number of tracks and the energy deposits in the hadronic and electromagnetic calorimeter. The algorithm may, however, fail for overlapping energy deposits. To solve this problem, we are itteratively removing from further consideration the energy deposits associated with an identified tau, and recalculate the isolation. This new definition of the isolation improves the reconstruction of the signal event with boosted topology and has a good discrimination power against QCD multi-jet events.

[1] L. Randall and R. Sundrum, Phys. Rev. Lett. **83** (1999) 3370.

[2] V. Khachatryan *et al.* [CMS Collaboration], *Search for massive resonances in dijet systems containing jets tagged as W or Z boson decays in pp collisions at sqrt(s)= 8 TeV*, arXiv:1405.1994 [hep-ex].

[3] K. Agashe, H. Davoudiasl, G. Perez *et al.*, Phys. Rev. D **76** (2007) 036006.

[4] S. D. Ellis, C. K. Vermilion, and J. R. Walsh, Phys.Rev. D81 (2010) 094023.

[5] J. Thaler and K. Van Tilburg, JHEP 1103 (2011) 015.

[6] CMS Collaboration [CMS Collaboration], *Identifying Hadronically Decaying Vector Bosons Merged into a Single Jet*, CMS-PAS-JME-13-006.

[7] L. Susskind, Phys. Lett. D **20** (1979) 2619.

[8] R. Contino,T. Kramer, M. Son and R. Sundrum, JHEP **1208** (2012) 013.

[9] D. Marzocca,M. Serone and J. Shu, JHEP **05** (2007) 074.

[10] T. Arrestad, *Comparison of b-tagging algorithms in CMS for jets with high transverse momenta containing multiple b quarks*, CMS AN-2014/076 (2014).

[11] C. Weiser, *A combined secondary vertex based B-tagging algorithm in CMS*, CERN-CMS-NOTE-2006-014.

[12] A. Rizzi, F. Palla and G. Segneri, *Track impact parameter based b-tagging with CMS*, CERN-CMS-NOTE-2006-019.

[13] the CMS Collaboration, *Particle flow Event reconstruction in CMS and Performance for Jets, Taus and Missing E_T*, CMS PAS PFT-09-001 (2009).

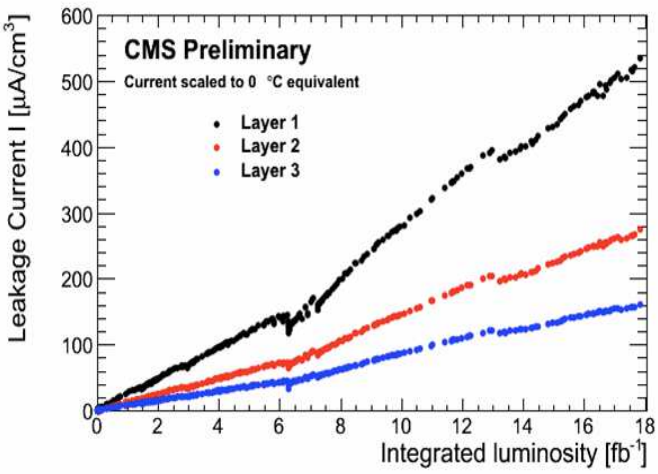

FIG. 13.12 – Leakage currents with integrated luminosity.

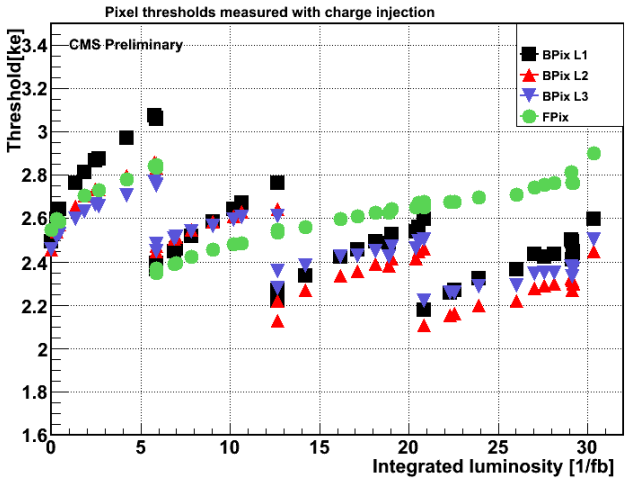

FIG. 13.13 – Pixel thresholds with integrated luminosity.

13.4 Detector maintenance, operations, and upgrades

The extremely high particle fluxes at small distances from the interaction point require the innermost tracking layers to be composed of pixel devices delivering spatial information with high resolution. Over the full acceptance of the CMS detector, the silicon pixel system provides two or more hits per track, which allow secondary vertices to be reconstructed for tagging long-lived objects, like b or c quarks and τ-leptons, and to distinguish them from a large background of light quark and gluon jets [1]. It is also an important detector for identifying the primary vertex, and separating it from dozens of additional pile-up vertices.

Our CMS group is dedicated to operating, maintaining, and upgrading the barrel pixel detector (BPIX), which the University of Zürich helped build. This detector plays a special role in our physics measurements since it is used in identifying b-quark jets which are in the final state of most of the physics analyses in our research portfolio. Our responsibilities are threefold:

- We maintain and operate the current BPIX which will be taking the first data at 13 TeV starting in the middle of 2015.

- We are helping to build the phase I upgraded BPIX detector for installation at the end of 2016.

- We have also started to work on the design and simulations for the phase II upgrade of the pixel detector which is envisioned to take data starting 2023.

13.4.1 Barrel pixel detector maintenance and operations

The Pixel Detector was installed in 2008 and showed excellent performance during the first LHC run. Nevertheless, it has been a subject to severe radiation damage, what resulted in such effects as increase of the leakage current (Fig. 13.12) and of the bias voltage, charge trapping and signal degradation, or changes in the pixel thresholds (Fig. 13.13). Hence, several corrections are needed in order to guarantee correct operation. Our group is responsible for calibrations aimed at finding the optimal settings for the irradiated detector (see Fig. 13.14), which is temporarily installed in the clean room of LHC-P5 (Cessy, France).

FIG. 13.14 –
Barrel pixel detector temporarily installed in P5.

The barrel pixel detector will record the first LHC collisions after the long shutdown in the middle of 2015 at higher instantaneous luminosities and at a center of mass energy of 13-14 TeV. BPIX and FPIX detectors were extracted in the middle of 2013 to allow access to the beam pipe and for the duration of the current long shutdown. The pixel detector was placed in a refrigerated, climate-controlled room environment located at the CMS experimental site, Point 5. BPIX is currently maintained in two cold boxes in a lab with repair workbenches, and all the electronics and computers necessary to control and readout the detector for tests. In coordination with PSI, who is leading the work on BPIX, our group has installed the DAQ system, and performed the necessary testing, and calibration of the BPIX modules. Our work included setting up the computers that are connected to the VME, as well as the software infrastructure needed to make such tests and calibrations.

The pixel detector has been operated with a coolant temperature of 7.4°C in 2008 - 2011 and 0°C in 2012, which for the pixel sensors translates to values ~ 10°C higher. In order to limit the impact of radiation damage and minimize the leakage current, during the second LHC run the detector must be operated at much lower temperature, down to -20°C. Since the working points and settings are strongly temperature dependent, during this year we performed calibrations down to -15°C, attempting to reach even lower values.

During the previous run 22 out of a total of 768 BPIX modules had problems. For FPIX the problematic fraction was even 7.7%. We have now helped replace and calibrate most of these modules and this job will be completed before the end of this summer. Moreover, two malfunctioning analog optical hybrids, needed to convert the electric analog signal from the readout chips to an optical analog signal for transmission through optical fibers to the readout electronics placed outside the detector. Both have been now replaced and tested.

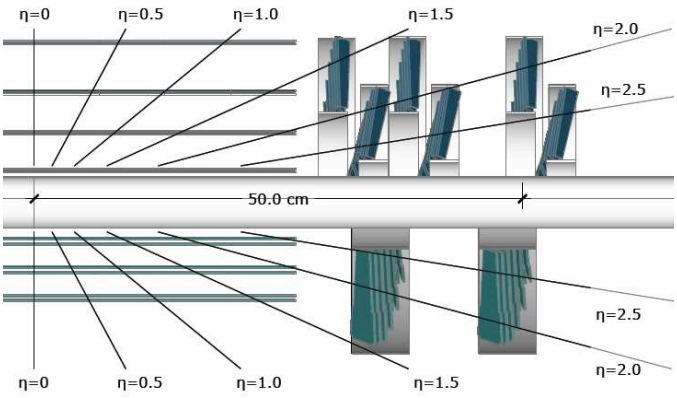

FIG. 13.15 – Schematic of barrel pixel upgrade. Bottom half represents current 3-layer BPIX system, top half shows upgraded 4-layer system in which the innermost detector plane is located within 3 cm of the beam axis.

During the shutdown, several updates to the computers and software have been implemented. Our group updated all the pixel detector online DAQ software packages from 32- to 64-bit and to the latest Scientific Linux version and its compiler. We updated the software version control system to allow for parallel development of several packages by different persons and cleaned up and removed outdated packages. We are developing a new graphical user interface for the control room DAQ system and calibration software, which will allow additional information to be displayed and further automatize the calibration software to enable remote access and control so that remote users will be able to do some levels of shift work.

13.4.2 Barrel pixel detector phase I upgrade

The current pixel detector is not designed for the expected LHC run 2 conditions of 2×10^{34} cm^{-2}s^{-1} at 50 ns. The phase 1 pixel upgrade [2] combines a new pixel readout chip with several other design improvements to keep up performance. The current 3-layer central pixel barrel, 2-disk forward pixel detectors are to be replaced with 4-layer central pixel barrel, 3-disk forward pixel detectors (Fig. 13.15).

The current BPIX detector consists of three 57 cm long layers of silicon pixel modules serviced by 2.2 m of supply tubes which transport cooling tubes, electrical power, and optical signals. The University of Zurich designed and constructed the mechanical support structure, and designed, built, and tested the supply tubes, including the mechanical structure, cooling and service lines, and boards to transfer optical signals (see Fig. 13.16). We are in charge of the phase I upgrade for these components. The additional inner pixel layer requires a complete redesign. To reduce the amount of dead material which has a negative impact on the detector performance a new, lightweight cooling system will be installed. We have now

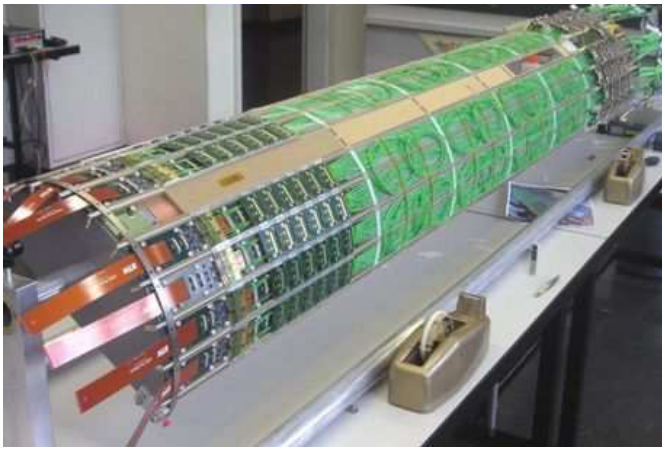

FIG. 13.16 – Current supply tube quarter, outfitted with electronics and cabling, produced at UZH.

constructed two prototype half-barrels of the four necessary for the phase I upgraded cooling structure; one can be seen in Sec. 19. These systems differ from the current system in that the tubes are much narrower, operate at 60 times higher pressure, are constructed in a complicated looping structure in order to cool more components including the newly added DC-DC converters, and use two-phase liquid-gas CO_2 cooling instead of single-phase C_6F_{14} liquid coolant. We have performed leak and deformation tests at 170 atmospheres, twice the operating pressure. The two prototypes are now at CERN for testing.

13.4.3 Beam tests of pixel detectors

We participated in tests of the prototype pixel sensors and frontend chips performed in October 2013 and March 2014 at the Fermi National Accelerator Laboratory. The "MT3 High Rate" tracking area provided 120 GeV protons or 66 GeV pions at intensities up to 4×10^8 /s. The setup consisted of two telescopes, each containing eight identical pixel sensors bump-bonded on readout chips (ROC). Seven planes were used for tracking and one plane as a detector under test (DUT). The first telescope had sensors perpendicular to the beam to test the saturation of time stamp buffer (single-pixel hits mostly), whereas in the second telescope sensors were inclined by 20° to simulate the deflection in the CMS magnetic field. In the latter situation the ionization charge is collected by more than one pixel resulting in a better position resolution.

Several issues were identified during these tests, such as the freezing of the double-column readout and other readout or out-of-sync errors. The former problem was understood as a too slow (above 25 ns) release of the signal used by pixels to notify the chip periphery of a valid hit resulting in spurious timestamps. The problem was resolved in the new ROC version (digV2.1) tested in March.

The hit residuals for the tilted DUT have a Gaussian width (σ) of 24 μm and 15 μm along the two coordinates, and preliminary efficiency measurements are above 98%. The data analysis is currently ongoing and a full understanding of the chip prototype is a prerequisite for the final mass production.

13.4.4 CMS Phase 1 System Test

The barrel pixel supply tube supports ten types of electronics boards which communicate with the pixel modules to handle control signals, power conversion (DC-DC converters) and distribution, data readout, electrical to optical signal conversions, communication with the DAQ, as well as the cooling loop structure. Our group is responsible for building the mechanical support structure, the cooling loop system, some of the electronics components, and the overall installation, integration and testing of the complete system, to be delivered to CERN for installation in 2016. For that purpose we are installing a full CMS-pixel DAQ system at the University of Zürich, commission it and write the necessary software. The system makes use of power supplies, control modules, a DCS system, readout electronics (FEDs), and two readout systems (VME until 2016, μTCA 2017 and after) as well as additional equipment to handle the complex fiber arrangements and to check the fiber connections.

The design of the new components of the control and data acquisition system is ongoing and first prototypes are being produced. We are currently setting up a slice of the full readout chain in order to gain experience in the operation of the new system and validate the individual components in view of the final production. The system will consist of a group of pixel detector modules connected through optical links to the front-end boards for readout and control and powered using a set of DC-DC converters. We have developed some tests of components of the power and control chain, but considerable work is still needed over the coming years to integrate all detector parts to a complete system and in the development of sophisticated software algorithms for testing, calibration and monitoring of all detector components.

13.4.5 Detector studies and hit reconstruction

Irradiation produces defects in silicon devices which cause trapping of charge carriers and modify the electric field profile across the sensor bulk. We studied charge collection in the CMS pixel sensors along their lifetime and as a function of the depth at which charge carriers are produced [4]. The study was based on CMS data collected in 2011 and 2012. During normal LHC operations the pixel sensors were biased at 150 V, however, small datasets were collected also with bias voltages between 70 and 300 V resulting in different Lorentz deflections.

Charge collection as a function of the sensor depth was studied using the grazing angle technique [5] which uses tracks crossing the sensors at shallow angles and releasing ionization charge over a long sequence of pixels, as shown in Fig. 13.17. The measured charge pro-

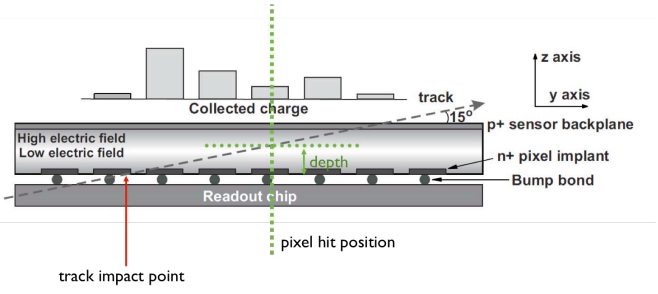

FIG. 13.17 – Sketch of the grazing angle technique

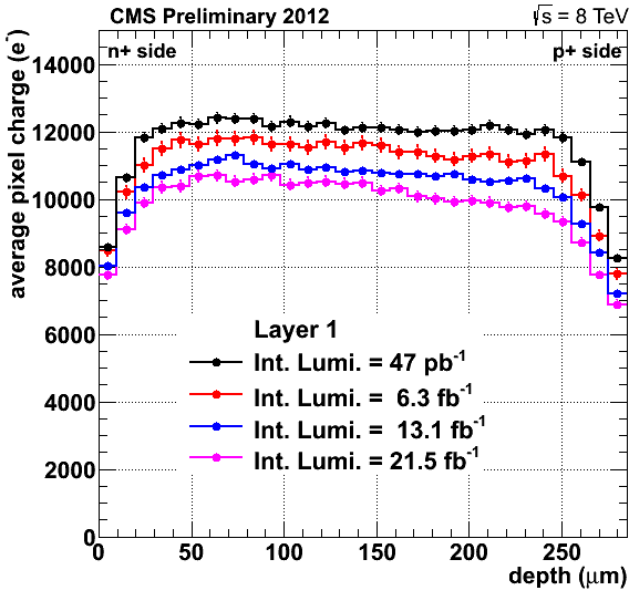

FIG. 13.18 – Average charge profiles as a function of the sensor depth for different integrated luminosities.

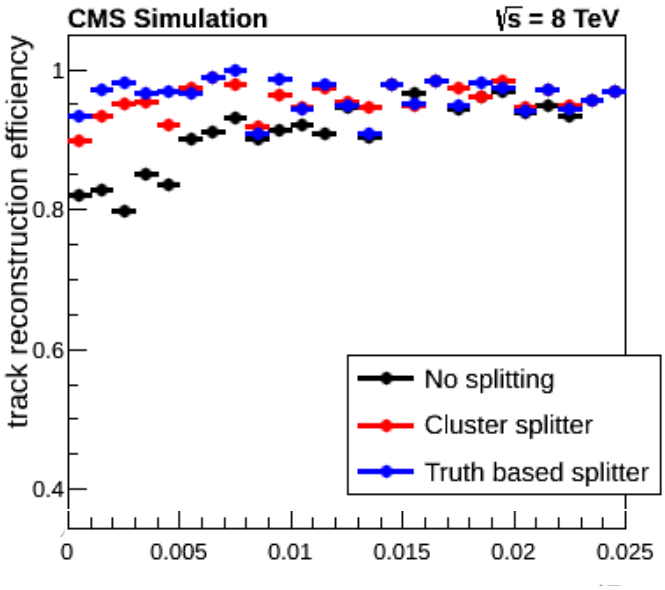

FIG. 13.19 – Track reconstruction efficiency versus angular separation, with and without pixel hit splitting.

files clearly demonstrateate a decrease of collected charge with increasing irradiation (Fig. 13.18). Moreover, charge losses are more pronounced at large depths, due to the long drift distance of charge carriers.

The charge profiles at different bias voltages and irradiations were compared with a detailed sensor simulation, PIXELAV [6–8], and are currently used to optimize our modeling of radiation damage. The PIXELAV simulation computes average cluster shapes, also called *templates*, used during pixel hit reconstruction.

We also worked on improving the reconstruction of pixel hits in narrow particle jets. When two charged particles traverse the sensors in close proximity, the pixel hits may merge into one larger cluster. In the innermost layer of the pixel detector hit overlap occurs if the opening angle between the two particle trajectories is below 5 mrad. For a typical three-prong τ decay this corresponds to a transverse momentum around 150 GeV/c.

Our group, in collaboration with Johns Hopkins University, has developed a technique for splitting merged clusters, which can be identified by the larger dE/dx and resolved by an algorithm that compares the observed cluster charge distribution with the expected template.

We have tested the algorithm in the new CMS tracking setup, imitating the harsh conditions of the 2015 LHC run. A simulated sample of $Z' \rightarrow 2\tau$ decays at $m_{Z'} = 1.5$ TeV was used. A significant increase in tracking efficiency is observed in Fig. 13.19 for tracks with angular separation dR$<$ 0.01. For three-prong τ decays at $p_T > 300$ GeV/c the reconstruction efficiency increases by typically 30%.

The algorithm is now integrated in the official CMS software framework and the necessary templates will soon be available from a central database. This way the evolving running conditions will be taken into account automatically and hit splitting will be performed in the distributed data processing.

[1] W. Erdmann (Paul Scherrer Institut), *The CMS pixel detector*, World Scientic Review (2009).

[2] *CMS technical design report for the pixel detector upgrade*, CMS collaboration, CERN-LHCC-2012-016.

[3] V. Khachatryan *et al.* [CMS Collaboration], CERN-LHCC-2012-016. CMS-TDR-11 (2012).

[4] S. Taroni [for the CMS collaboration], Proceedings of the 2013 IEEE-NSS symposium. CMS CR-2013/096.

[5] Y. Allkofer *et al.*, Nucl. Instrum. Meth. A **584** (2008) 25.

[6] M. Swartz, Nucl. Instrum. Meth. A **511** (2003) 88-91.

[7] V. Chiochia *et al.*, IEEE Trans. Nucl. Sci. **52** (2005) 1067-1075.

[8] M. Swartz *et al.*, Nucl. Instrum. Meth. A **565** (2006) 212-220.